Supplementary Materials: Fast and Simultaneous Determination of Soil Properties using Laser-induced Breakdown Spectroscopy (LIBS): A Case Study of Typical Farmland Soils in China

Xuebin Xu [1,2], Changwen Du [1,2,*], Fei Ma [1], Yazhen Shen [1] and Jianmin Zhou [1]

[1] State Key Laboratory of Soil and Sustainable Agriculture, Institute of Soil Science, Chinese Academy of Sciences, Nanjing 210008, China
[2] University of Chinese Academy of Sciences, Beijing 100049, China
* Correspondence: chwdu@issas.ac.cn; Tel.: +86-25-86881565

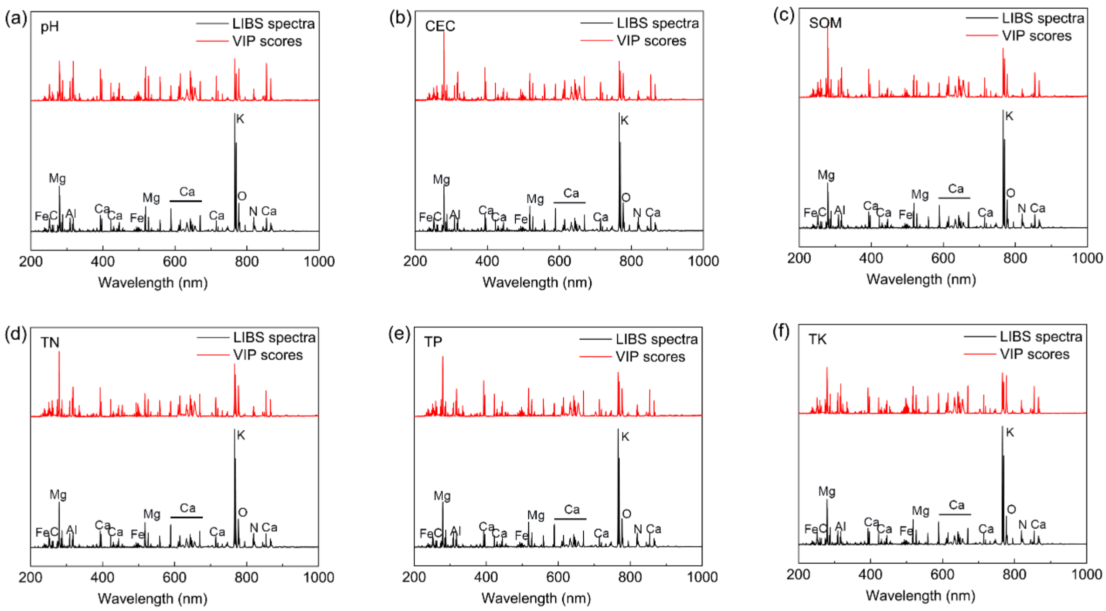

Figure S1. Variable importance in the projection (VIP) scores for the prediction of (a) pH, (b) CEC, (c) SOM, (d) TN, (e) TP, and (f) TK using PLSR model.

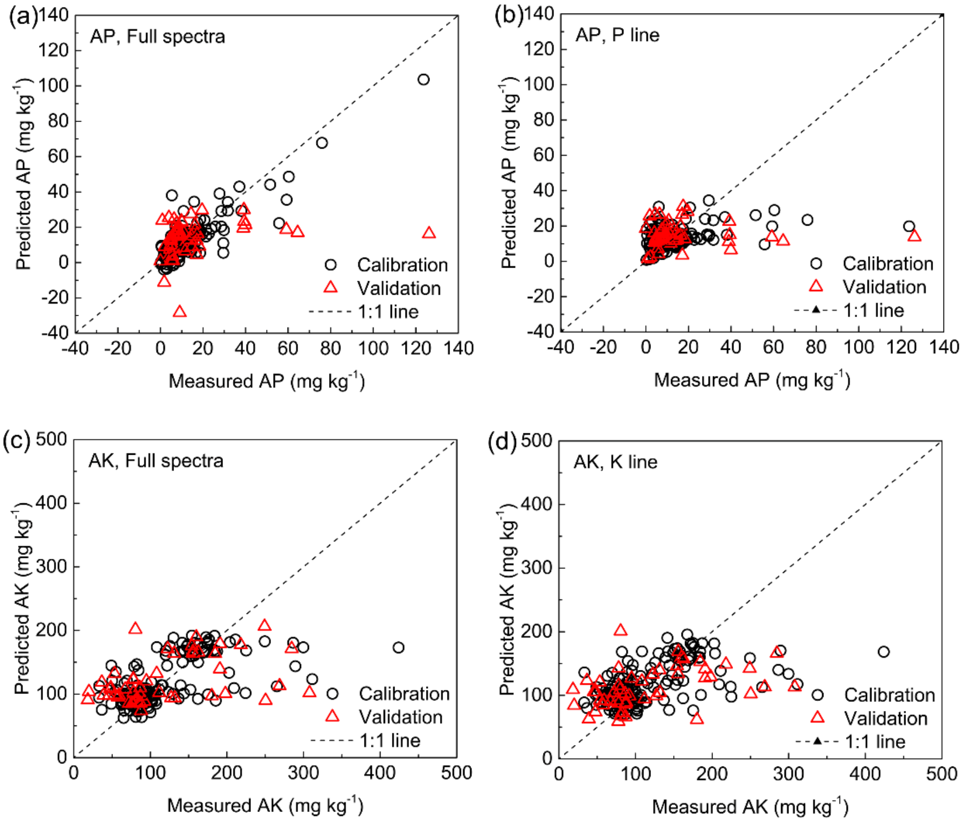

Figure S2. Scatterplots of measured values versus predicted values of soil available P (a, b) and available K contents (c, d) using the PLSR model based on the full and characteristic LIBS spectra.

Table S1. The detailed information of the sampling sites.

Soil type	Sampling position	Land usages	Climatic conditions
Fluvo-aquic soil	116°22′–116°45′ E, 36°40′–37°12′ N	Wheat-corn crop rotation	Monsoonal climate, with mean annual temperature and precipitation of 13.1 °C and 593 mm
Paddy soil	119°22′–121°00′ E, 30°54′–32°01′ N	Rice-rapeseed crop rotation	Subtropical humid monsoon climate, with mean annual temperature and precipitation of 15.7 °C and 1100 mm
Red soil	116°20′–116°51′E, 28°2′–28°30′ N; 117°26′–118°00′ E, 27°48′–28°24′ N	Paddy fields, forests, orchards, and tea plantation	Subtropical humid monsoon climate, with mean annual temperature and precipitation of 17.7 °C and 1712 mm
Black soil	126°14′–127°45′ E, 46°58′–47°52′ N; 126°16′–127°53′ E, 47°35′–48°33′ N	Crop corn and soybean	Temperate continental monsoon climate, with mean annual temperature and precipitation of 1–2 °C and 500–600 mm

Table S2. Identification of the LIBS emission lines based on the *NIST Atomic Spectra Database* and previous literatures.

Elements	**Observed wavelength (nm)**	**References**
C	247.8 (247.5–249.5)	247.8 nm in soil [1, 2]
		247.9 nm in soil [3] and fly ash [4]
O	777.1 (773.4–782.9)	777.00 nm according to NIST Atomic Spectra Database [5]
	794.6 (791.6–801.6)	794.717 nm in silicon wafer [6]
	655.6 (649.7–664.3), 844.6 (840.2–848.3)	844.625 and 655.6068 nm according to NIST Atomic Spectra Database [5]
N	343.75 (343.2–344.6);	343.72 and 460.72 nm in sand [7]
	460.5 (459.8–460.9)	
	742.3, 744.2, 746.8 (739.4–755.3)	742.36, 744.23, 746.83 nm in sand [7] and soil [8]
	818.25, 819.3, 821.7, 824.3 (815.6–828.0)	818.4, 818.8, 821, 824 nm in N-rich molecules [9]
P	253.7 (253.1–254.4)	253.6 and 255.5 nm in gel [10] and soil [11]
	440.2 (439.4–440.6)	440.2104 nm according to NIST Atomic Spectra Database [5]
K	766.3, 769.8 (762.6–772.8)	766.49 and 769.95 nm in cement powder [12] and mars soil [13]
Na	588.7, 589.3 (587.60–591.10)	588.99 and 589.59 nm in water [14], vegetables [15] and steel [16]
Ca	422.5 (420.3–423.9)	422.672 nm in meat [17]
	445.3 (443.6–446.1)	445.48 nm in vegetables [15]
	487.5 (487.2–488.0)	487.81 nm in cigarette [18]
	558.55 (557.7–560.6)	558.88 nm in cigarette [18]
	315.7, 317.7 (314.3–320.5)	315.887 and 317.933 nm in cigarette [18]
	373.5 (372.8–376.9)	373.69 nm in cigarette (Ahmed et al. 2017)
	393.0, 396.5 (391.5–399.5)	393.367 nm in engine oils [19]

	866 (861–867)	866.214 nm according to NIST Atomic Spectra Database [5]
	849.6 (848.0–850.4)	849.802 nm in cigarette [18]
	854.0 (852.1–856.2)	854.209 nm in cigarette [18]
Mg	279.3, 280.0 (276.90–282.60)	279.553 nm in milk [20];
		279.55 nm in cement powder [12];
		279.5 nm in residue [21];
		280.2 nm in engine oils [19]
	285.0 (284.20–285.70)	285.218 nm in mars surface [22];
		285.21 nm in aluminum sample [23];
		285.213 nm in metallic [24]
	382.9, 383.50 (380.8–384.4)	383.829 nm in aluminum alloys [25, 26]
	517.0 (516.7–517.6)	517.268 nm according to NIST Atomic Spectra Database [5]
	518.10 (517.6–519.6)	518.37 nm in vegetables [15]
Al	257.40 (256.9–257.8)	257.51 nm in residue [21]
	309.2 (303.9–312.2)	309.27 nm in engine oils [19] and cement powder [12],
Si	250.55, 251.45 (249.5–255.2)	250.69 nm in water [27];
		251.61 nm in vegetables [15]
	287.90 (286.2–290.1)	288.16 nm in cement powder [12] and aluminum sample [23]
		288.158 nm in metallic [24];
		288.2 nm in residue [21]
Fe	259.7, 260.5 (254.4–263.3)	259.936 nm in engine oils [19];
		259.940 nm in metallic [24]

Table S3. Summarized prediction ability of soil available P and available K by various spectroscopic technique in previous studies.

Reference	Model	Spectroscopic technique	Extraction method	Prediction ability
[28]	PLSR	Vis-NIR	NH_4F-HCl extractable–P	R_V^2 = 0.29; $RMSE_V$ = 19.33 mg/kg; RPD_V = 1.17
			NH_4OAC extractable–K	R_V^2 = 0.07; $RMSE_V$ = 20.82 mg/kg; RPD_V = 0.77
[29]	RF	MIR	Mehlich-3 extractable–P	R^2 = 0.51; RMSE = 0.4 $cmol_c$/kg
			Mehlich-3 extractable–K	R^2 = 0.49; RMSE = 0.4 $cmol_c$/kg
		TXRF	Mehlich-3 extractable–P	R^2 = 0.10; RMSE = 966 mg/kg
			Mehlich-3 extractable–K	R^2 = 0.16; RMSE = 895 mg/kg
[30]	PLSR	Vis/NIR-DRF	CAL extractable–P	R_{CV}^2 = 0.54; $RMSE_{CV}$ = 0.05 g/kg
			CAL extractable–K	R_{CV}^2 = 0.15; $RMSE_{CV}$ = 0.05 g/kg
[31]	PLSR	VIS	Colwell (P)	R_{CV}^2 = 0.06; $RMSE_{CV}$ = 4.94 mg/kg
			NH_4OAC extractable–K	R_{CV}^2 = 0.29; $RMSE_{CV}$ = 2.02 mg/kg
		NIR	Colwell P	R_{CV}^2 = 0.01; $RMSE_{CV}$ = 4.91 mg/kg
			NH_4OAC extractable–K	R_{CV}^2 = 0.47; $RMSE_{CV}$ = 1.82 mg/kg
		MIR	Colwell P	R_{CV}^2 = 0.20; $RMSE_{CV}$ = 5.24 mg/kg
			NH_4OAC extractable–K	R_{CV}^2 = 0.38; $RMSE_{CV}$ = 1.92 mg/kg
[32]	SAM–PLSR	PAS	NH_4OAC extractable–P	R_V^2 = 0.45; $RMSE_V$ = 40.45 mg/kg; RPD_V = 0.82
		ATR	NH_4OAC extractable–P	R_V^2 = 0.49; $RMSE_V$ = 34.75 mg/kg; RPD_V = 0.97
		DRF	NH_4OAC extractable–P	R_V^2 = 0.50; $RMSE_V$ = 48.79 mg/kg; RPD_V = 0.81

References

1. Cremers, David A., Michael H. Ebinger, David D. Breshears, Pat J. Unkefer, Susan A. Kammerdiener, Monty J. Ferris, Kathryn M. Catlett, and Joel R. Brown. Measuring total soil carbon with laser-induced breakdown spectroscopy (LIBS). *J. Environ. Qual.*, **2001**, *30*, 2202-2206.
2. Ebinger, Michael H., M. Lee Norfleet, David D. Breshears, David A. Cremers, Monty J. Ferris, Pat J. Unkefer, Megan S. Lamb, Kelly L. Goddard, and Clifton W. Meyer. Extending the applicability of laser-induced breakdown spectroscopy for total soil carbon measurement. *Soil Sci. Soc. Am. J.*, **2003**, *67*, 1616-1619.
3. Martin, Madhavi Z., Stan D. Wullschleger, Charles T. Garten, and Anthony V. Palumbo. Laser-induced breakdown spectroscopy for the environmental determination of total carbon and nitrogen in soils. *Appl. Opt.*, **2003**, *42*, 2072-2077.
4. Noda, M., Y. Deguchi, S. Iwasaki, and N. Yoshikawa. Detection of carbon content in a high-temperature and high-pressure environment using laser-induced breakdown spectroscopy. *Spectrochim. Acta, Part B*, **2002**, *57*, 701-709.
5. A. Kramida, Y. Ralchenko, J. Reader, and NIST ASD Team. NIST Atomic Spectra Database (Ver. 5.6). Gaithersburg National Institute of Standards and Technology, 2012.
6. Ji, Zhen Guo, Jun Hua Xi, and Qi Nan Mao. Determination of oxygen concentration in heavily doped silicon wafer by laser induced breakdown spectroscopy. *J. Inorg. Mater.*, **2010**, *25*, 893-895.
7. Harris, Ronny D., David A. Cremers, Michael H. Ebinger, and Brian K. Bluhm. Determination of nitrogen in sand using laser-induced breakdown spectroscopy. *Appl. Spectrosc.*, **2004**, *58*, 770-775.
8. Dong, D. M., C. J. Zhao, W. G. Zheng, X. D. Zhao, and L. Z. Jiao. Spectral characterization of nitrogen in farmland soil by laser-induced breakdown spectroscopy. *Spectrosc. Lett.*, **2013**, *46*, 421-426.
9. De Lucia Jr, Frank C., and Jennifer L. Gottfried. Characterization of a series of nitrogen-rich molecules using laser induced breakdown spectroscopy. *Prop. Explos. Pyrotech.*, **2010**, *35*, 268-277.
10. Aras, Nadir, and Şerife Yalçın. Rapid identification of phosphorus containing proteins in electrophoresis gel spots by laser-induced breakdown spectroscopy, LIBS. *J. Anal. At. Spectrom.*, **2014**, *29*, 545-552.
11. Lu, Cuiping, Liusan Wang, Haiying Hu, Zhong Zhuang, Yubing Wang, Rujing Wang, and Liangtu Song. Analysis of total nitrogen and total phosphorus in soil using laser-induced breakdownspectroscopy. *Chin. Op. Lett.*, **2013**, *11*, 053004.
12. Mansoori, A., B. Roshanzadeh, M. Khalaji, and S. H. Tavassoli. Quantitative analysis of cement powder by laser induced breakdown spectroscopy. *Opti. Laser. Eng.*, **2011**, *49*, 318-323.
13. Sallé, Béatrice, David A. Cremers, Sylvestre Maurice, Roger C. Wiens, and Pascal Fichet. Evaluation of a compact spectrograph for in-situ and stand-off laser-induced breakdown spectroscopy analyses of geological samples on Mars missions. *Spectrochim. Acta, Part B*, **2005**, *60*, 805-815.
14. Giacomo, A. De, M. Dell'Aglio, F. Colao, R. Fantoni, and V. Lazic. Double-pulse LIBS in bulk water and on submerged bronze samples. *Appl. Surf. Sci.*, **2005**, *247*, 157-162.
15. Juvé, Vincent, Richard Portelli, Myriam Boueri, Matthieu Baudelet, and Jin Yu. Space-resolved analysis of trace elements in fresh vegetables using ultraviolet nanosecond laser-induced breakdown spectroscopy. *Spectrochim. Acta, Part B*, **2008**, *63*, 1047-1053.
16. Xiao, X., S. Le Berre, K. C. Hartig, A. T. Motta, and I. Jovanovic. Surrogate measurement of chlorine concentration on steel surfaces by alkali element detection via laser-induced breakdown spectroscopy. *Spectrochim. Acta, Part B*, **2017**, *130*, 67-74.

17. Velioglu, Hasan Murat, Banu Sezer, Gonca Bilge, Süleyman Efe Baytur, and Ismail Hakki Boyaci. Identification of offal adulteration in beef by laser induced breakdown spectroscopy (LIBS). *Meat Sci.*, **2018**, *138*, 28-33.
18. Ahmed, Nasar, Zeshan A. Umar, Rizwan Ahmed, and M. Aslam Baig. On the elemental analysis of different cigarette brands using laser induced breakdown spectroscopy and laser-ablation time of flight mass spectrometry. *Spectrochim. Acta, Part B*, **2017**, *136*, 39-44.
19. Yaroshchyk, Pavel, Richard J. S. Morrison, Doug Body, and Bruce L. Chadwick. Quantitative determination of wear metals in engine oils using laser-induced breakdown spectroscopy: A comparison between liquid jets and static liquids. *Spectrochim. Acta, Part B*, **2005**, *60*, 986-992.
20. Abdel-Salam, Z., J. Al Sharnoubi, and M. A. Harith. Qualitative evaluation of maternal milk and commercial infant formulas via LIBS. *Talanta*, **2013**, *115*, 422-426.
21. Zheng, Hongbo, Fang Yu Yueh, Tracy Miller, Jagdish P. Singh, Kristine E. Zeigler, and James C. Marra. Analysis of plutonium oxide surrogate residue using laser-induced breakdown spectroscopy. *Spectrochim. Acta, Part B*, **2008**, *63*, 968-974.
22. Sallé, Béatrice, Jean-Luc Lacour, Evelyne Vors, Pascal Fichet, Sylvestre Maurice, David A. Cremers, and Roger C. Wiens. Laser-induced breakdown spectroscopy for Mars surface analysis: capabilities at stand-off distances and detection of chlorine and sulfur elements. *Spectrochim. Acta, Part B*, **2004**, *59*, 1413-1422.
23. Sabsabi, Mohamad, Vincent Detalle, Mohamed A. Harith, Walid Tawfik, and Hisham Imam. Comparative study of two new commercial echelle spectrometers equipped with intensified CCD for analysis of laser-induced breakdown spectroscopy. *Appl. Opt.*, **2003**, *42*, 6094-6098.
24. Ismail, Marwa A., Gabriele Cristoforetti, Stefano Legnaioli, Lorenzo Pardini, Vincenzo Palleschi, Azenio Salvetti, Elisabetta Tognoni, and Mohamed A. Harith. Comparison of detection limits, for two metallic matrices, of laser-induced breakdown spectroscopy in the single and double-pulse configurations. *Anal. Bioanal. Chem.*, **2006**, *385*, 316-325.
25. Rai, Awadhesh K., Hansheng Zhang, Fang Yu Yueh, Jagdish P. Singh, and Arel Weisberg. Parametric study of a fiber-optic laser-induced breakdown spectroscopy probe for analysis of aluminum alloys. *Spectrochim. Acta, Part B*, **2001**, *56*, 2371-2383.
26. Li, Hong Kun, Ming Liu, Zhi Jiang Chen, and Run Hua Li. Quantitative analysis of impurities in aluminum alloys by laser-induced breakdown spectroscopy without internal calibration. *Trans. Nonferr. Met. Soc. China*, **2008**, *18*, 222-226.
27. Gondal, M. A., and T. Hussain. Determination of poisonous metals in wastewater collected from paint manufacturing plant using laser-induced breakdown spectroscopy. *Talanta*, **2007**, *71*, 73-80.
28. Ji, Wenjun, Zhou Shi, Jingyi Huang, and Shuo Li. In situ measurement of some soil properties in paddy soil using visible and near-infrared spectroscopy. *PLoS One*, **2014**, *9*, e105708.
29. Towett, Erick K., Keith D. Shepherd, Andrew Sila, Ermias Aynekulu, and Georg Cadisch. Mid-infrared and total X-ray fluorescence spectroscopy complementarity for assessment of soil properties. *Soil Sci. Soc. Am. J.*, **2015**, *79*, 1375-1385.
30. Udelhoven, Thomas, Christoph Emmerling, and Thomas Jarmer. Quantitative analysis of soil chemical properties with diffuse reflectance spectrometry and partial least-square regression: A feasibility study. *Plant Soil*, **2003**, *251*, 319-329.
31. Viscarra Rossel, R. A., D. J. J. Walvoort, A. B. McBratney, L. J. Janik, and J. O. Skjemstad. Visible, near infrared, mid infrared or combined diffuse reflectance spectroscopy for simultaneous assessment of various soil properties. *Geoderma*, **2006**, *131*, 59-75.

32. Ma, F., C. W. Du, J. M. Zhou, and Y. Z. Shen. Investigation of soil properties using different techniques of mid-infrared spectroscopy. *Eur. J. Soil Sci.*, **2018**, *70*, 96–106.